

SIMULATION OF URBAN-SCALE DISPERSION USING A LAGRANGIAN STOCHASTIC DISPERSION MODEL

MATHIAS W. ROTACH

Climate Research ETH, Winterthurerstr. 190, CH-8057 Zürich, Switzerland

(Received in final form 4 October 2000)

Abstract. Based on recent knowledge concerning the vertical structure of turbulence statistics within the roughness sublayer (i.e., the layer directly influenced by individual roughness elements) over urban surfaces the problem of urban-scale dispersion is studied. On this scale it is impossible to resolve each roughness element so that the rough character of the surface has to be taken into account by introducing a roughness sublayer, which is generally not present in dispersion models even when employed in urban environments. Two types of simulations are presented here: one, called 'urban', takes into account the roughness sublayer's turbulence structure, while the other, 'non-urban', does not. A brief overview is given on what changes are required for an 'urban' simulation as compared to a 'non-urban' or standard dispersion simulation. In particular, a parameterisation is proposed for the vertical profile of Reynolds stress within the roughness sublayer.

Using a Lagrangian stochastic particle dispersion model 'urban' and 'non-urban' simulations are compared for a variety of boundary-layer states and different source configurations. It is found that neglecting the roughness sublayer results in the largest errors for low source heights and under conditions of mechanically dominated turbulence. This is of particular importance due to the fact that urban surfaces tend to increase the mechanical portion of turbulence and, in addition, low sources, such as traffic and domestic heating, are predominant in urban environments.

On the basis of three tracer data sets from urban release experiments it is shown that, in general, the 'urban' simulation improves the model performance yielding smaller fractional bias at the same time as the normalised mean square error is reduced and the correlation to the observations is increased. This indicates that indeed the physical description of the dispersion process is better taken into account in the 'urban' simulation. For stable stratification the above statement does not hold true either due to other processes masking the roughness-sublayer influence in this regime or, alternatively, due to a failure of the similarity relations for the turbulence statistics under extremely stable stratification.

Keywords: Air pollution, Particle model, Roughness sublayer, Turbulence, Urban dispersion.

1. Introduction

Urban air pollution is an environmental problem of major concern and will, due to growing urbanisation, probably become increasingly important. The definition and evaluation of abatement strategies often require predictions of pollutant modelling. It is a fact that air pollution is a typically urban problem, yet little is known concerning the flow and dispersion characteristics over urban surfaces. Usually, dispersion simulations in urban areas are performed using the same numerical models as over the countryside with minor modifications such as the selection of



a larger value for the roughness length (e.g., Kono, 1997). In a similar fashion Gaussian dispersion models are 'adapted' to urban conditions by replacing the empirical relations describing the plume width and depth (σ_y and σ_z , respectively) as a function of the distance from the source by respective urban counterparts (e.g., Hanna, 1982). In this study it will be argued that modifications of this kind are not likely to capture the essential features of urban dispersion characteristics. In particular, the flow and turbulence characteristics of the roughness sublayer (i.e., the layer directly influenced by the roughness elements, see below) have to be taken into account.

In simulations of ground level concentrations over urban surfaces it is often found that these are underpredicted as compared to observed values. Olesen (1995) compares operational dispersion models (Gaussian, puff and hybrid models). All the involved models underpredict near-surface concentrations from the Copenhagen tracer experiment (Gryning and Lyck, 1994) by 20 to 50% and from the Lillestrøm tracer experiment (Haugsbakk and Tønnesen 1989) by 40 to 120%. Both these tracer experiments were performed over suburban surfaces. Underpredictions at the lower end of the range given for the operational models, or somewhat less, result from simulations with a one-dimensional Lagrangian stochastic particle dispersion model (Tassone et al., 1994), a two-dimensional particle model (Rotach et al., 1996) or the puff-particle model (PPM) of de Haan and Rotach (1998) for the Copenhagen data set. In a dispersion study over the Athens area using the TVM mesoscale model (Schayes et al., 1996) in combination with an Eulerian approach for simulating dispersion of pollutants, Martilli et al. (1997) found that the primary pollutants were underpredicted, especially during the night.

In a numerical experiment using a Lagrangian stochastic particle dispersion model (LSPDM), Rotach (1997a) shows that the underprediction of surface concentrations is likely to be due to neglecting the flow and turbulence structure of the urban roughness sublayer (RS). The practical applicability of explicitly taking into account the RS is demonstrated by Rotach and de Haan (1997), who again use an LSPDM for the Copenhagen tracer experiment and find that the underprediction of the surface concentrations can be resolved for their 'urban type' simulation (i.e., when taking into account the RS, see below). De Haan et al. (1998a) arrive at similar conclusions when using a Gaussian dispersion model for Copenhagen and also for the simulation of yearly average surface concentrations over the city of Zurich, Switzerland (de Haan et al., 2000). For the Lillestrøm tracer experiment, finally, the results for the crosswind-integrated concentration also improve when invoking the 'urban type' simulation (Rotach, 1999).

In Section 2, the most important features of the flow and turbulence characteristics of the urban RS are briefly summarised. In particular, a new parameterisation for the Reynolds stress profile within the RS, which takes into account all the available observations, is presented. Section 3 gives an overview on the model used in the present study and 'urban' and 'non-urban' types of simulations are introduced. In Section 4 a sensitivity analysis is presented showing under which conditions the

proposed ‘urban’ approach differs most markedly from the traditional ‘non-urban’ approach. In Sections 5 and 6 it is shown that the consideration of RS characteristics improves the prediction of surface concentrations in the case of two out of the three available tracer experiments over urban areas. Section 7, finally, places the results into perspective and discusses needs for future research.

2. The Urban Roughness Sublayer

2.1. STRUCTURE

In simulating the flow (and dispersion) over an urban surface, two basic approaches can be followed:

- Numerically compute the detailed flow field by reducing the spatial (and hence temporal) resolution of the model to an order of one metre or even less in order to explicitly resolve each of the roughness elements (buildings, trees, ...).
- Assume a horizontally averaged flow field by treating the surface as (extremely) rough by introducing a *roughness sublayer* (RS), i.e., a lowest layer adjacent to the surface, wherein the flow is determined through the height and distribution of the roughness elements.

The first approach, while physically most reliable, is obviously limited for urban-scale applications by its excessive demand on computing time and the requirements concerning detailed information on building structure. In contrast to this the second approach has certainly an advantage (and will be followed in this study), but requires information on the influence of usually tall, solid and densely grouped roughness elements on average flow characteristics. In the present study we follow the suggestion of Raupach et al. (1991) in defining the vertical extent of the RS as ranging from the physical surface ($z = 0$) up to a height z_* , the RS height. This definition explicitly includes the *urban canopy layer* (UCL) as a part of the RS. Above the RS the flow can be considered in equilibrium with the rough surface (given a large enough urban settlement) and the influence of individual roughness elements has vanished due to turbulent mixing. This layer is called the *inertial sublayer* (IS) and it corresponds to the upper part of the *surface layer* (SL), which is usually assumed to cover the lowest ten percent of the boundary layer over surfaces with lesser roughness. For simulations with tall roughness elements and comparably low boundary-layer height, no true matching layer, i.e., no IS, may exist between the RS and the urban mixed layer/ stable boundary layer (Rotach, 1999). Estimates for z_* are often expressed as multiples of h , the average roughness element height, or alternatively, as a function of h and D , where D is the average spacing between roughness elements. Raupach et al. (1991) in a review article conclude that $z_* = 2h - 5h$ essentially covers the range of estimates from the literature concerning vegetated surfaces (stemming, however, mostly from wind-tunnel experiments). For urban surfaces no systematic estimates are available to

the knowledge of the author. Rotach (1993a) presents evidence that his highest measurement level over the city of Zurich, Switzerland at $z/h = 2.1$ is probably within the RS and similar findings are reported by Roth and Oke (1993) for their level at $z/h = 2.6$. These few pieces of evidence indicate that the broad range given by Raupach et al. (1991) is probably also valid for urban surfaces. However, further research may reveal more detail, especially on the dependence of z_* on the density and distribution of roughness elements over real urban surfaces.

2.2. TURBULENCE STRUCTURE WITHIN THE URBAN ROUGHNESS SUBLAYER

It is beyond the scope of the present paper to give an exhaustive overview over the turbulence characteristics close to urban surfaces. For this the reader is referred to, e.g., Roth (2000). Rather, two important points will be made here, which are particularly relevant for problems in connection with dispersion modelling. Firstly, it has been observed in a number of relatively recent field studies that turbulent fluxes, and in particular Reynolds stress, are not ‘approximately constant with height’ (as would be expected in the SL over surfaces of lesser roughness). Rather, $\overline{u'w'}$ (i.e., its norm) appears to increase with height within the RS before reaching an approximately constant value in the IS (Rotach, 1993a; Oikawa and Meng, 1995; Feigenwinter et al., 1999). A parameterisation for the height dependence of $\overline{u'w'}$ has been proposed by Rotach (1993a). However, due to its mathematical formulation, its evaluation is crucially sensitive to how closely $\overline{u'w'}(z)/\overline{u'w'}^{IS} = 1$ is assumed to be reached at $z = z_*$. Here, $\overline{u'w'}^{IS}$ refers to the presumably constant value of Reynolds stress in the IS. As a basis for a more general parameterisation Figure 1 shows a conceptual sketch of Reynolds stress as a function of height over an urban surface. Rather than increasing towards a maximum in absolute values at the ground, $(\overline{u'w'}_o)$, as over smoother surfaces, the observations of Oikawa and Meng (1995), Rafailidis (1997) and Feigenwinter et al. (1999) indicate that a maximum in the correlation between horizontal and vertical velocity fluctuations is reached *at a certain distance* from the surface. Below this level, Reynolds stress (i.e., its magnitude) decreases again and assumes a value close to zero at the zero plane displacement height ($z = d$, Rotach, 1993a). It is argued here that the height of maximum correlation may serve as a surrogate for z_* and likewise the maximum observed Reynolds stress must be close to the (approximately constant) inertial sublayer value, $\overline{u'w'}^{IS}$.

The Reynolds stress reduction close to the roughness as suggested by Figure 1, is most likely due to additional (form) drag exerted on the flow by the blunt roughness elements. Martilli et al. (2000), using a simple parameterisation for this term in the momentum balance of their numerical model, show that the essential features of observed Reynolds stress profiles are reproduced. However, the question arises, as to why the maximum Reynolds stress (in magnitude) occurs well above $z = h$, in contrast to other rough surfaces like plant canopies, where the maximum is observed at the ‘top of the canopy’, i.e., $u_{*0}^2 = -\overline{u'w'}(z = h)$ (Raupach et

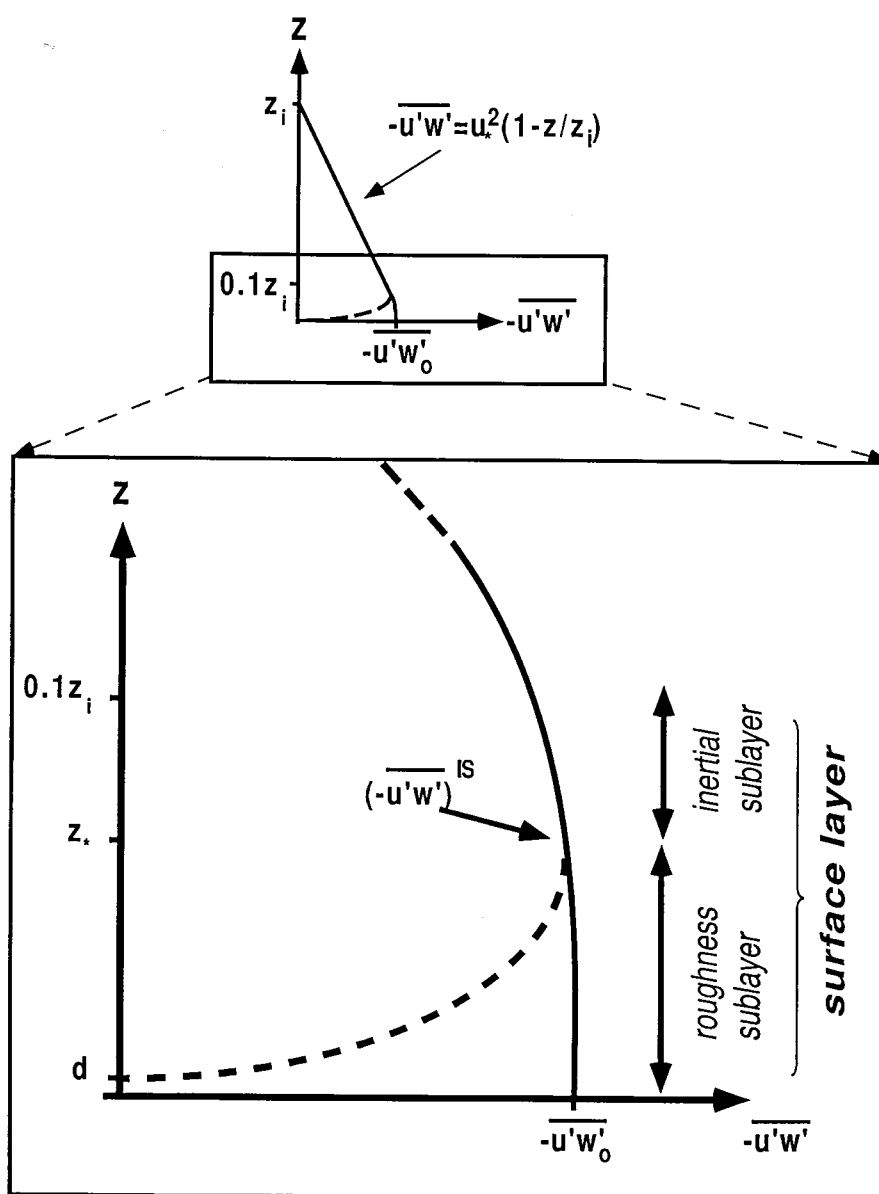


Figure 1. Conceptual sketch of Reynolds stress in the urban boundary layer. The solid line corresponds to a parameterisation according to de Haan and Rotach (1998), which slightly departs from the ‘standard’ linear profile (cf. the upper part of the figure) in that it assumes an approximately constant value when approaching the surface.

al., 1991). The difference lies in the canopy structure of a typical urban surface. Often, building heights are not uniform within the footprint (Schmid, 1997) of an observation or model grid point, so that the *average* building height, $z = h$, is not the uppermost level, up to which form drag acts. In principle, this level corresponds to the height of the highest obstacle within the footprint, but the latter may have only a minor influence. Thus, the height of maximum Reynolds stress is dependent on the height-distribution of roughness elements. In their simulations Martilli et al. (2000) have successfully used $z_* = h + \Delta z$, where Δz is the standard deviation of the distribution of obstacle heights.

It should be noted that Figure 1, although being different to standard text book knowledge concerning Reynolds stress profiles close to the surface at the first glance, is not at odds with this knowledge after a closer look. Raupach et al. (1991) have pointed out that the RS may be considered the rough-wall counterpart to the viscous sublayer over smoother surfaces. Due to the laminar character of the latter, turbulent velocity fluctuations and hence their correlation must vanish within the viscous sublayer and the ‘surface value’ of Reynolds stress (or other turbulence statistics of the SL) turns out to be a pure extrapolation (see also Rotach, 1993a).

In Figure 2 the data from the available full-scale studies and a wind-tunnel experiment are plotted in the scaling framework as suggested by Figure 1. The average building heights for the three full-scale data sets are 18.3 m (Rotach, 1993a), 7 m (Oikawa and Meng, 1995) and 24 m (Feigenwinter et al., 1999), respectively. The height of the maximum Reynolds stress is estimated at $z/h = 3$ from the data of Rotach (1993a) and observed at $z/h = 1.47$ (Oikawa and Meng, 1995) and $z/h = 2.1$, respectively. Considering the differences in the surface structure among the various sites the scatter is extremely low. The solid line in Figure 2 corresponds to

$$\left(\frac{u_{*,l}(z)}{u_*^{\text{IS}}} \right)^b = \sin \left(\frac{\pi}{2} Z \right)^a, \quad Z \leq 1 \quad (1)$$

where $u_{*,l}(z) = (-\overline{u'w'}(z))^{1/2}$ is the local friction velocity, $Z = z'/z'_*$ is a non-dimensional height using $z' = z - d$ and $z'_* = z_* - d$. The parameters a and b are fitted to the data of Figure 2 to yield $a = 1.28$ and $b = 3.0$. The parameter fit is performed using only the full-scale data, yielding a rms difference between observations and the fitted curve of 0.052 ($n = 8$ data points). Including the wind-tunnel data of Rafailidis (1997) for $B/h = 1/2$ (see caption of Figure 2) does not largely change the obtained parameter values ($a = 1.26$, $b = 3.66$), while his data for $B/h = 1$ are slightly off the curve as obtained from the full-scale studies.

In his wind-tunnel study Rafailidis (1997) has investigated the effect of roof shape on the turbulence characteristics of the (urban) RS. Regular arrays of ‘buildings’ with slanted roofs yield Reynolds stress profiles with a much larger peak close to roof level than Figure 1 suggests and the data from these experiments do not fit the parameterisation (1). Likewise, Rotach (1993a) and Feigenwinter et al.

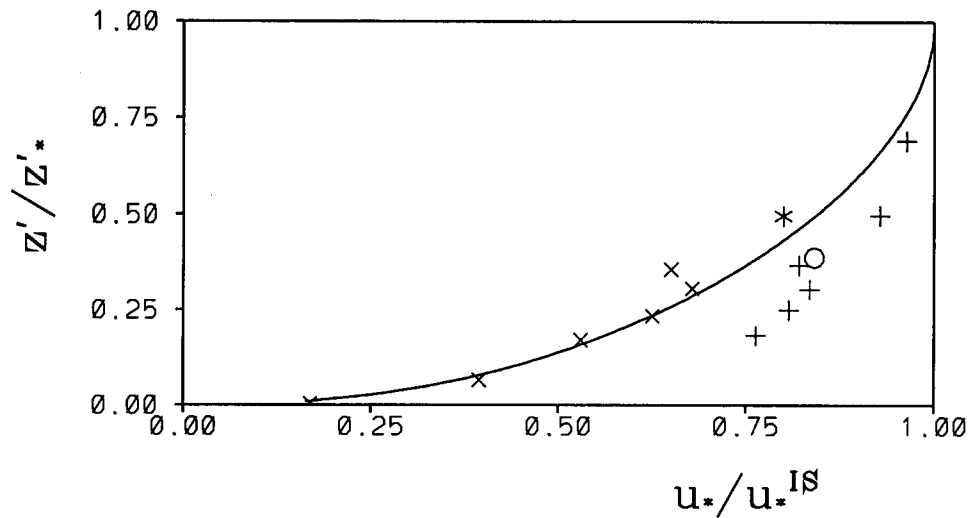


Figure 2. Parameterised profile of (local) friction velocity, u_* , as a function of non-dimensional height, Equation (1). The symbols refer to the full-scale data of Rotach (1993a), x ; Oikawa and Meng (1995), $*$ and Feigenwinter et al. (1998), o . Wind-tunnel data after Rafailidis (1997), $+$, are shown for comparison. The latter are not employed to fit the parameters in Equation (1) (only the 'flat roof' experiments with aspect ratio 1/2 shown).

(1999) report a certain stability dependence of the shape of their Reynolds stress profiles. This indicates that a parameterisation of the type (1) will require further refinement with respect to detailed surface morphology and/or stability, once more data are available. Nevertheless, due to the lack of better knowledge at present, Equation (1) will be used in this study for those simulations that explicitly take into account the turbulence characteristics of the RS (see below). Other turbulent fluxes, such as sensible and latent heat, are likely to also vary with height within the urban RS (Rotach, 1991). However, very little systematic information concerning their behaviour is available in the literature, so that in the following simulations their value is held constant throughout the urban RS.

A direct consequence of the height variation of Reynolds stress as outlined above is the need for a scaling framework for, e.g., the velocity variances within the RS to be used in dispersion simulations. Two different approaches may be considered to obtain a 'friction velocity', i.e., a scaling velocity that accounts for the mechanical part of turbulence kinetic energy production: the inertial sublayer friction velocity, u_*^{IS} , could be used having the advantage to be one characteristic scale throughout the RS. However, Rotach (1993b) has shown that this scaling approach yields inferior results as compared to the alternative one, i.e., local scaling. The success of local scaling has already been demonstrated earlier (Högström et al., 1982) and later in a number of field studies (e.g., Roth and Oke, 1993; Oikawa and Meng, 1995; Feigenwinter et al., 1998). Note that 'local scaling' here does not refer to the theoretical framework of Nieuwstadt (1984) for the stable boundary layer

with all its assumptions and implications. Rather, the field studies indicate that if $u_{*,l}$ is used many of the ‘classical’ SL relations according to Monin–Obukhov similarity theory can be retained, sometimes even with the same parameter values. In the dispersion simulations below, local scaling in this weaker sense is invoked within the RS by combining the ‘usual SL-relations’ with Equation (1) to obtain the local friction velocity. Details of the treatment of individual variables can be found in Rotach (1997a, b).

3. Model Description and Definition of Simulations

3.1. THE LAGRANGIAN STOCHASTIC PARTICLE DISPERSION MODEL

The simulations presented below are performed using a LSPDM. This type of model is not only regarded as the most advanced type of dispersion model, it is also perfectly suited for the present task because ‘average’ turbulence characteristics can easily be modified according to the simulated situation. The present model is based on the two-dimensional LSPDM of Rotach et al. (1996) but is extended to three dimensions as described in de Haan and Rotach (1998). The basic feature of the model is that it fulfils the well-mixed condition (Thomson, 1987) continuously between jointly Gaussian turbulence on the one hand, and a flow with skewed vertical velocity and the fluctuating velocity components being uncorrelated on the other hand. This property is achieved by modelling the probability density function (pdf), P , of the (Eulerian) velocity components as

$$P = F P_u P_v P_c + (1 - F) P_g, \quad (2)$$

where P_u and P_v are Gaussian distributions in the longitudinal (u) and lateral (v) velocity components, respectively; P_c is a positively skewed distribution in the vertical velocity component (w) that is constructed from two Gaussians and corresponds to the one-dimensional pdf of Luhar and Britter (1989); P_g is a three-dimensional Gaussian pdf that is formally written here as

$$P_g = P_u P_v P_w P_{uw} \quad (3)$$

in order to emphasise the fact that the correlation between v and w is neglected while P_{uw} describes that between u and w (see Rotach et al., 1996 for the exact formulations of these Gaussian distributions). The function F in (2) is used to model the smooth transition between different turbulent states of the boundary layer. If $F = 0$ the pdf is simply a three-dimensional Gaussian distribution with u and w being correlated, while for $F = 1$ the velocity components are uncorrelated and, in particular, the distribution in the vertical velocity is skewed. Essentially, F is modelled as a function of the Obukhov length, L , the convective velocity scale, w_* , and height z , thereby ensuring that $F \rightarrow 1$ for increasing instability, and $F \rightarrow 0$ for

near-neutral and stable conditions (and thus also when approaching the surface). For details of its functional form see Rotach et al. (1996). In a purely neutral or stable boundary layer F is zero throughout the whole height range, and under highly convective conditions F only deviates from one very close to the surface, and in a situation of forced convection F starts at zero near the ground, increases throughout the middle third of the boundary layer and assumes a value of one higher up.

Based on the velocity pdf (2) the Fokker–Planck equation is solved in the usual manner ensuring the well-mixed condition (Thomson, 1987) is fulfilled. For the purely Gaussian limiting case the model reduces to the solution of Thomson (1987) and to obtain the solution in the limit $F \rightarrow 1$ the one-dimensional formulation of Luhar and Britter (1989) is used (Rotach et al., 1996). The stochastic part of the velocity accelerations is modelled using the structure function in the inertial subrange (Thomson, 1987). The universal constant in this formulation, C_o , is set to three according to the most recent estimates (Du et al., 1995; Rotach et al., 1996; Du, 1997).

Concentration fields are determined using the kernel method (de Haan, 1999), rather than by box counting, so that fewer particles have to be released for every simulation. De Haan (1999) points out that most of the concentration features can be captured with as few as 5,000 particles but the details close to the source such as the steep rise and the distance where it begins may require more. Therefore, in the sensitivity simulations (Section 4) 15,000 particles are released due to the necessity to capture the concentration patterns close to the source. For the simulation of the tracer experiments in Sections 5 and 6, on the other hand, the first arcs are sufficiently far away from the source that only 5,000 particles are employed.

3.2. ‘URBAN’ AND ‘NON-URBAN’ SIMULATIONS

Two types of simulations will be compared in the following:

- In the ‘*urban*’ simulations, a roughness sublayer is taken into account with a parameterised profile of Reynolds stress (Equation (1)). Accordingly, the concept of local scaling is applied to determine the remaining variables of interest within the RS (for details, see Rotach and de Haan, 1997 and Rotach, 1997b).
- In the ‘*non-urban*’ simulations the lower portion of the boundary layer is parameterised according to Monin–Obukhov similarity, therefore assuming that surface-layer characteristics prevail down to the ground. Thus, these simulations correspond to what is common practice for dispersion modelling even over urban surfaces (note that ‘non-urban’ does not mean rural, but rather the absence of an RS).

In both types of simulations, the profiles of the mean wind speed, the velocity variances, Reynolds stress and the dissipation rate of turbulent kinetic energy in the upper part of the boundary layer (i.e., above $0.1z_i$, where z_i is the boundary-layer height) are parameterised using appropriate (and equal) scaling relations dependent

on stability (i.e., z/z_i and z/L). Their exact functional forms together with data supporting them can be found in Rotach et al. (1996). As a friction velocity, u_*^{IS} is used to scale the velocity variances and the dissipation rate. The profile of mean wind speed is treated as follows. In the ‘non-urban’ simulation, for which a roughness length is specified ($z_o = 1$ m in the sensitivity runs of Section 4, or according to the observed values in Section 5) the non-dimensional gradient of mean wind speed is numerically integrated upward from $z = z_o$ throughout the boundary layer using the similarity formulation of Sorbjan (1986). In the ‘urban’ simulation on the other hand, the so calculated (i.e., ‘non-urban’) wind speed at $z = z_*$ is input. The numerical integration is then performed upward as well as downward (now using the local Reynolds stress to derive the local friction velocity). Rotach (1993a) shows that this way of determining the profile of mean wind speed within the RS yields an excellent agreement to observed profiles at an urban site in Zurich (Switzerland).

The same general approach is used for all other variables within the RS in the ‘urban’ simulations. Identical parameterisations are used as for the ‘non-urban’ approach, but now the *local friction velocity* according to (1) is employed for scaling purposes. Roth (2000) shows, on the basis of data from various full-scale observations, that this concept of local scaling captures the essential features of turbulence statistics in the urban RS. However, when approaching the surface, local scaling together with the decreasing Reynolds stress (Equation (1)) leads to vanishing standard deviations of the velocity components, σ_i as $z' \rightarrow 0$. This is at odds with observations (Rotach, 1995), which indicates that the σ_i/u_*^{IS} assume a constant value in the lower part of the RS. Therefore, the standard deviations of the velocity components are constrained to $\sigma_i \geq c_i u_*^{\text{IS}}$, where the c_i correspond to the observed values (Rotach, 1997a).

Figure 3 shows the parameterised ‘urban’ and ‘non-urban’ profiles of mean wind speed, the vertical and longitudinal velocity variances and the dissipation rate for a neutral boundary layer (stability B of Table I below). All these variables can be seen to be essentially identical above the IS while considerable deviations can occur within the RS. In this example, the velocity variances are constrained only at the lower most level in the ‘urban’ simulation. Note also that the ‘urban’ profile of mean wind speed is similar to that observed in the RS over other types of rough surfaces (Raupach et al., 1991; Rotach, 1993a).

4. Sensitivity

4.1. SIMULATIONS

In Table I four different stability regimes are defined through the friction velocity, u_* , the convective velocity, w_* , the boundary-layer height, z_i , and the Obukhov length, L . For each of these stability regimes a ‘non-urban’ simulation is performed

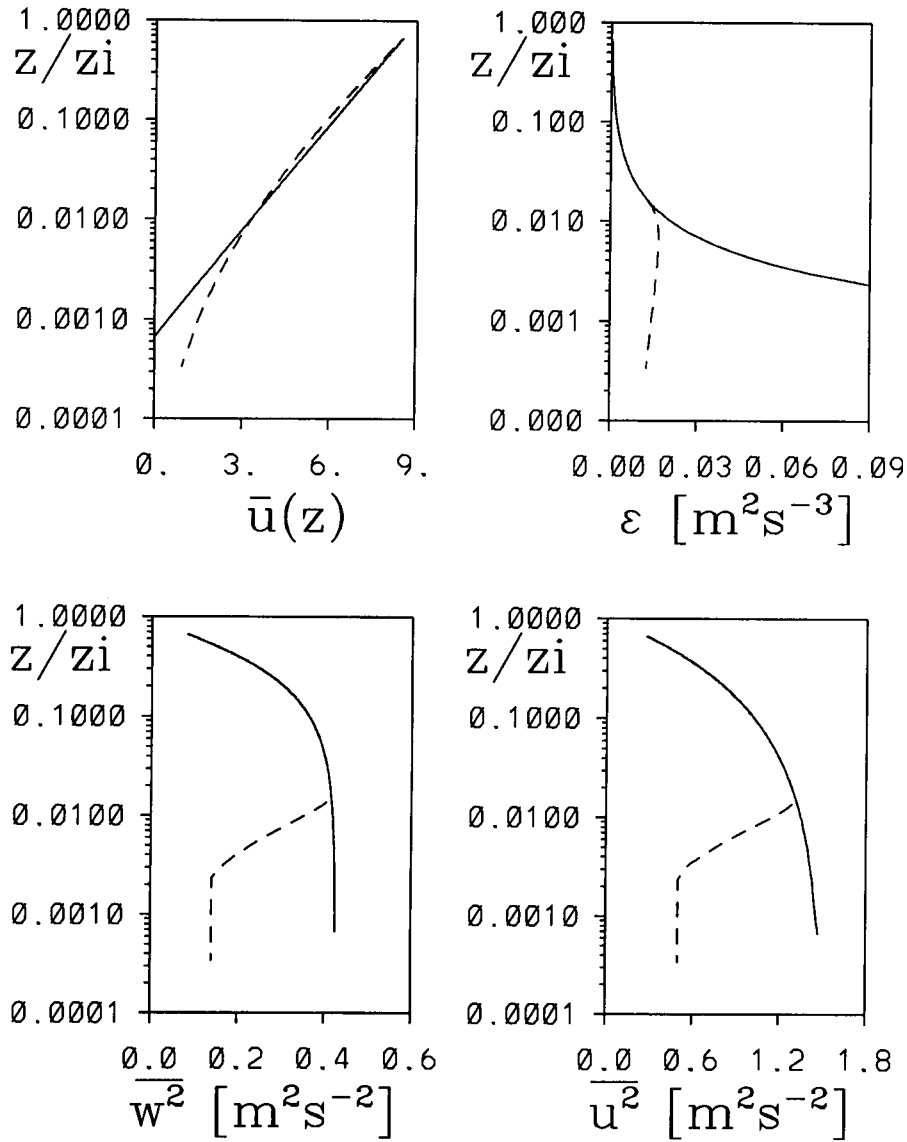


Figure 3. Profiles of turbulence statistics for 'urban' (dashed lines) and 'non-urban' (solid lines) simulations.

as well as a number of 'urban' simulations with varying parameters (see below). For the former, the roughness length, z_o is assumed as 1 m and particles are reflected at $z_r = 1.5$ m, i.e., 0.5 m above the 'ground'. In the 'urban' simulations, where the roughness length is not required, the particles are correspondingly reflected at $z_r = 0.5$ m, i.e., also 0.5 m above the 'ground'. Due to the fact that Reynolds stress is height dependent in the 'urban' simulations, u_* from Table I corresponds in these cases to the value in the inertial sublayer, u_*^{IS} . Four different source heights

TABLE I

Definition of boundary-layer parameters for the four stability regimes A–D.

Stability	u_* [m s ⁻¹]	w_* [m s ⁻¹]	z_i [m]	L [m]
A	0.3	–	396	200
B	0.5	–	1500	9999
C	0.2	1.0	1000	–20
D	0.2	2.0	1500	–3.75

are simulated for each of the stability categories (A to D) of Table I, namely $z'_s = 5/25/50/75$ m, respectively, where $z' = z - d$. It should be noted that in the ‘urban’ simulations the lower-most source height at 5 m may correspond to a source within the canopy, i.e., below the average building height for some of the values of the zero plane displacement height (see below).

For the ‘urban’ simulations a reference case is defined as follows. The average height of the roughness elements, h , is assumed at $h = 20$ m and the zero plane displacement d , is $d = 15$ m, i.e., ‘ $d/h = 0.75$ ’. This latter value closely corresponds to frequently suggested rule-of-the-thumb estimates (e.g., Grimmond and Oke, 1999; Rotach, 1994). In the ‘urban’ reference case the height of the roughness sublayer, z_* , is set to $z_*/h = 2$, i.e., at the lower end of the range as suggested by Raupach et al. (1991). In a sensitivity analysis both the zero plane displacement ($d/h = 0.25/0.5/0.75$) and the height of the roughness sublayer ($z_*/h = 2/3/4$) are varied for all categories of stability and all source heights. This yields a total of 80 simulations in the ‘urban’ mode.

Surface concentrations (the crosswind integrated concentration, CIC, the maximum on the arc, ArcMax and the lateral spread, SigY) are determined on equidistant arcs ($\Delta x = 60$ m) up to 1500 m from the source.

4.2. STABILITY AND SOURCE HEIGHT

In this section the results from the ‘non-urban’ and the ‘urban’ reference simulations are compared for all stabilities and source heights. Figure 4 summarises the results for neutral stability (regime B, Table I). The characteristics for CIC and ArcMax (not shown) are very similar: for all source heights the turbulence structure of the RS leads to higher peak concentrations, which have a tendency to occur somewhat farther downstream than in the ‘non-urban’ simulation (e.g., CIC for $z_s = 25$ m, Figure 4a). Clearly, the increase in surface concentration is the more pronounced the lower the source height is and can become very large at some few hundred metres downwind of a roof-level source ($z_s = 5$ m). This increase is due to the profile of Reynolds stress within the roughness sublayer, in

connection with the local scaling approach for, e.g., the velocity variances leading to a suppressed level of dispersion in the ‘urban’ simulations. Note again, that this reduction occurs *in comparison to the present ‘non-urban’ simulation*, in which (wrongly) surface-layer scaling is assumed to hold throughout the roughness sublayer and not in comparison to the conditions over rural surfaces! For large source heights the effect of roughness-sublayer turbulence on surface concentrations is still visible and systematic, albeit much smaller. In correspondence to the behaviour of CIC and ArcMax, the horizontal plume width is generally slightly smaller in the ‘urban’ simulation than in the ‘non-urban’ equivalent (Figure 4b) for a given source height. However, the urban modifications influence the relative magnitude of SigY: in the ‘non-urban’ simulations the highest source has the smallest lateral dispersion and the source height itself has only a minor effect on SigY, except for the very lowest, which is substantially larger than the others. In contrast, differences are generally larger in the ‘urban’ simulation and the relative order is reversed. The lowest source has now the smallest lateral dispersion, reflecting again the reduced velocity variance levels within the RS due to the Reynolds stress profile and the associated local scaling approach.

For the stable stratification (stability A) the effect of the RS is generally somewhat larger than for stability B but the relative differences between ‘urban’ and ‘non-urban’ simulations look similar (not shown). For the other two stability regimes of Table I, forced convection (C) and free convection (D), the effects of roughness-sublayer turbulence are relatively small (not shown). In both cases, differences between the two types of simulations can be substantial (i.e., similar in magnitude as in Figure 4) only for the roof level source ($z_s = 5$ m). For the higher sources, the ‘urban’ simulations exhibit some 20% (stability C) and 10% (D) larger concentrations at maximum.

Over all, we may summarise that the effect of the turbulence structure within the roughness sublayer on surface concentrations is substantial for stable and near-neutral stratification and/or for sources in the vicinity of roof level. For low sources the enhancement factor (due to RS turbulence) may easily be as large as three (all stability regimes) in the vicinity of the source and remains large under stable stratification relatively far downwind. Note that small source heights (chimneys, traffic) are very common in urban areas.

4.3. ROUGHNESS-SUBLAYER DIMENSIONS

Figure 5 depicts the surface concentrations for the various source heights and assumptions for z_* under stability B (Table I). The ‘urban effect’ is the more pronounced the higher the roughness sublayer becomes, i.e., the longer the travel distance of the plume is within the RS. The peak of the CIC (Figure 5a) is somewhat weaker and further downstream in a deeper RS. In addition the surface concentration far downstream of the source can be substantially larger if $z_* = 4h$ as compared to the reference simulation with a shallower RS. The maximum concen-

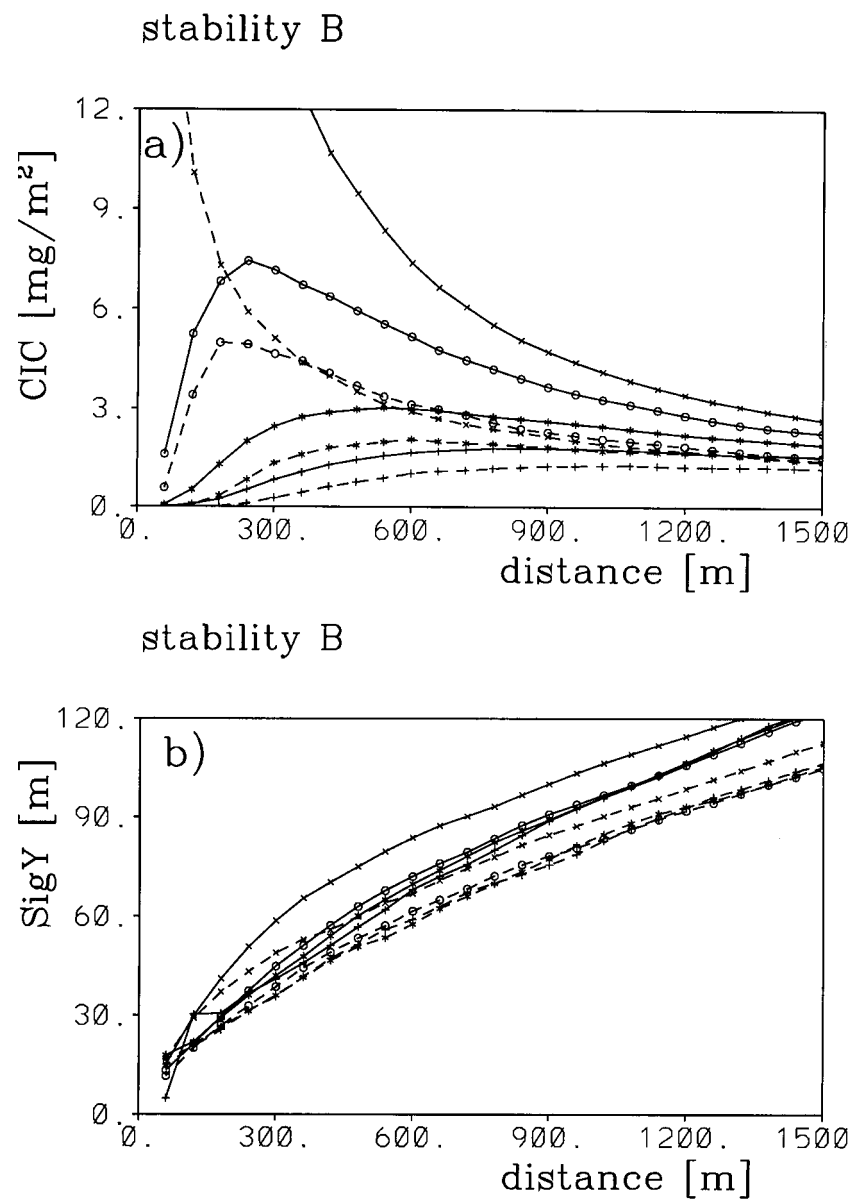


Figure 4. CIC (a), and SigY (b) for 'urban' (solid lines) and 'non-urban' (dashed lines) simulations under stability regime B (neutral) as a function of distance from the source. x: source height, $z_s = 5$ m, o: $z_s = 25$ m, *: $z_s = 50$ m, +: $z_s = 75$ m.

trations on the arcs (ArcMax, Figure 5b) correspond to this picture with similar modifications to the position of the peak and the roll-off as for CIC. The width of the plume (Figure 5c), finally, grows more rapidly in a deeper RS due to the larger layer with a reduced Reynolds stress and the corresponding (locally scaled) smaller velocity statistics. It is interesting to note that the linear portion of the increase in lateral plume width lasts much longer the deeper the RS becomes. According to the theory of Taylor (1921) this is the case for travel times much smaller than the Lagrangian integral time scale, T_L . For the present flow the relevant time is a local decorrelation time scale rather than T_L (Thomson, 1987) but nevertheless the results indicate this local decorrelation time scale to increase due to the urban modification in the present approach. Clearly, these characteristics are similar for all source heights investigated. However, substantial differences between surface concentrations are only observed if the source height is smaller than, or on the order of the height of, the roughness sublayer, z_* . In general, the described behaviour leads to higher surface concentrations close to the source in the case of a shallow RS and vice versa for the deeper RS. The ‘crossover’ occurs at about 13 times the source height for sources outside or at the upper end of the RS and substantially further downstream if the source is located deep within the roughness sublayer.

For stability A the influence of the RS height is similar albeit somewhat more pronounced as for the reference stability B (not shown). This reflects the stronger influence of mechanical turbulence on the dispersion characteristics under stable conditions. As for the ‘urban’–‘non-urban’ comparison (Section 4.1), the importance of z_* is relatively weak under conditions of forced convection and almost absent for the free convection case.

The influence of the zeroplane displacement length, d , is generally very similar in nature to that in z_* (not shown). A smaller d , in the present simulations, leads to a larger vertical extent of the RS (for z_*/h held constant) on the one hand and to (slightly) modified profiles of flow variables within the RS on the other hand.

Over all, the influence of RS dimensions (through z_* or d) can be substantial and amount to several ten percent if expressed as the difference relative to the ‘urban’ reference simulation. Given the fact that both these variables under consideration can not be determined with very high precision (Grimmond and Oke, 1999) this underlines the need for better methods to estimate z_* and d over urban areas. However, it should be noted that the respective differences between surface concentrations from ‘urban’ and ‘non-urban’ simulations are always much larger than those within the various ‘urban’ assumptions.

5. Application to Urban Tracer Data

‘Urban’ and ‘non-urban’ simulations are performed for three tracer data sets from release experiments over urban surfaces, namely those in Copenhagen, Lillestrøm and Indianapolis. Rotach and de Haan (1997) and Rotach (1997c), but using a

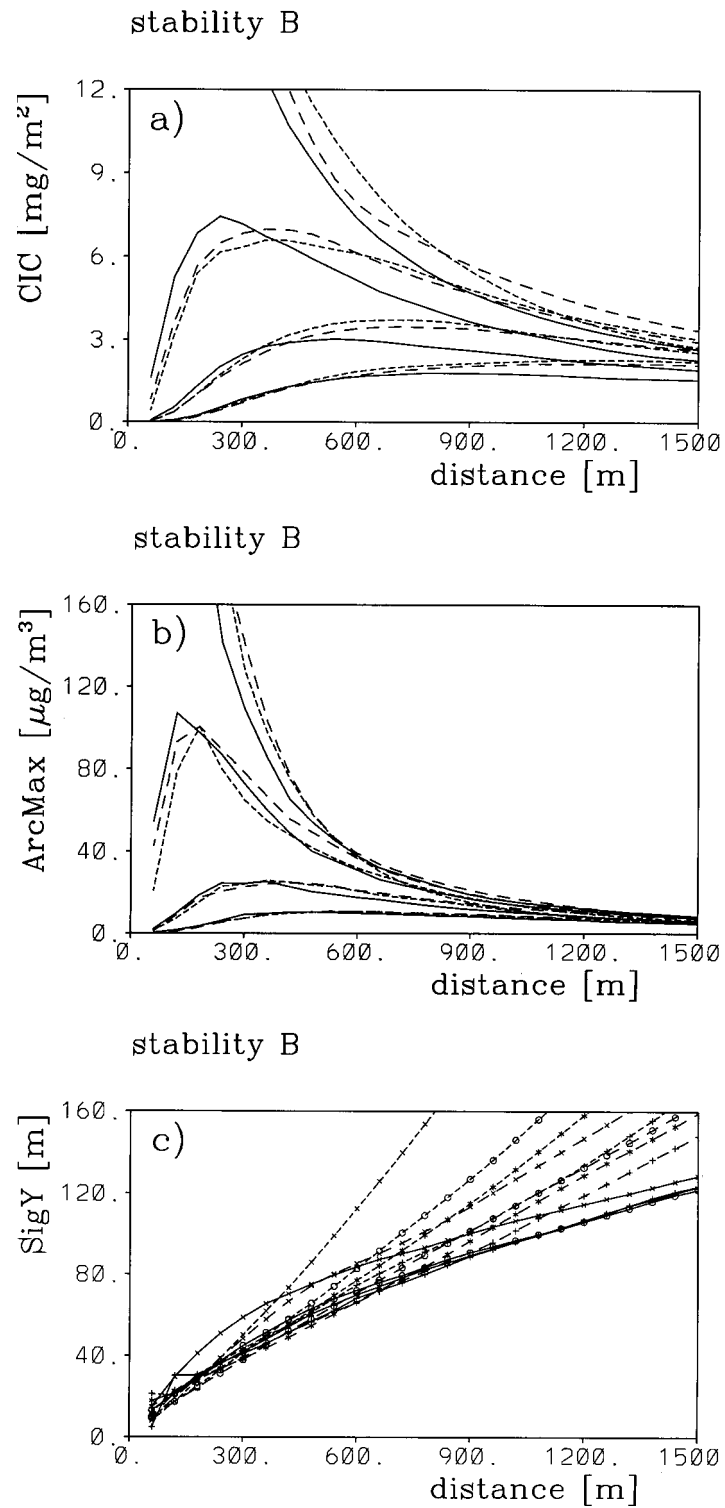


Figure 5. CIC (a), ArcMax (b) and SigY (c) for 'urban' reference ($z_* = 2h$, solid lines), $z_* = 3h$ (long dashed lines) and $z_* = 4h$ (short dashed lines) simulations under stability regime B (neutral) as a function of distance from the source. In (a) and (b) the lowest triple of curves corresponds to $z_s = 75$ m, the highest to $z_s = 5$ m and the intermediate triples accordingly. In (c) the symbols are as in Figure 4.

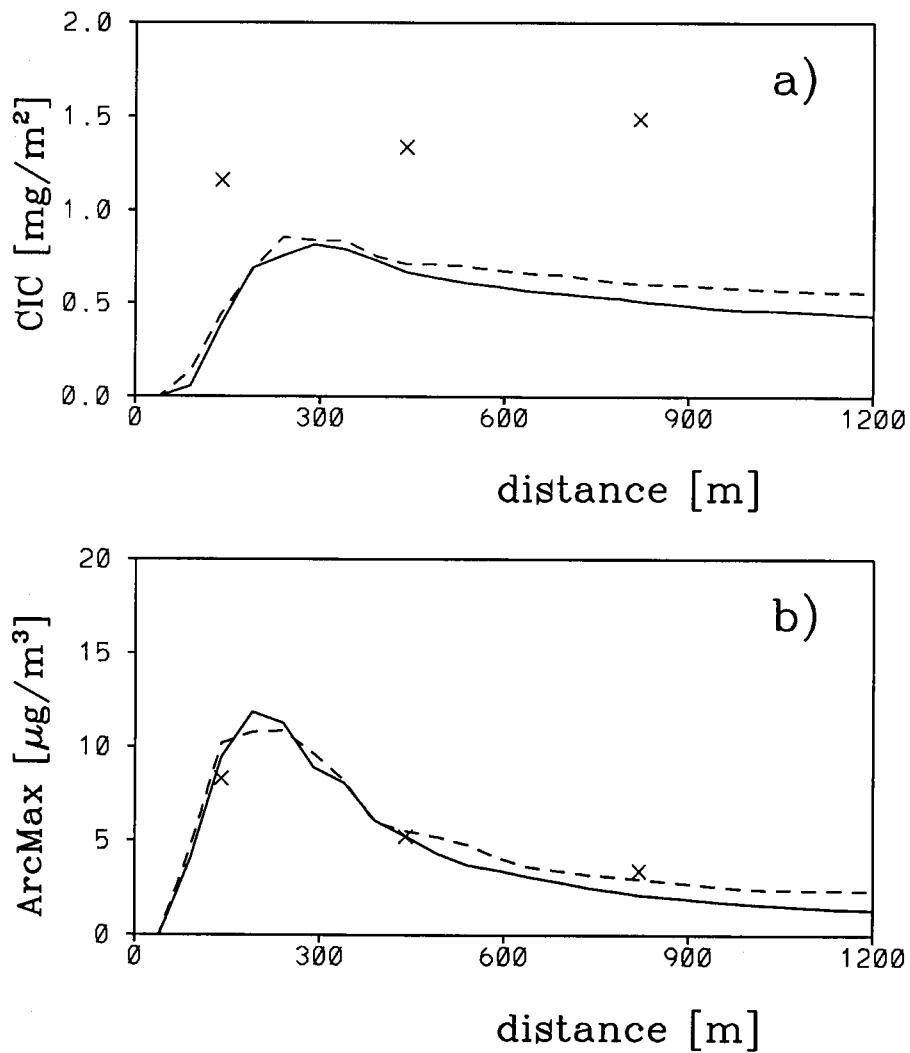


Figure 6. Surface CIC (a) and ArcMax (b) as a function of the distance from the source for the Lillestrøm release of January 10, 1987, 0945 hrs. dashed line: 'urban' simulation, solid line: 'non-urban' simulation.

two-dimensional LSPDM, have already simulated the Copenhagen and Lillestrøm experiments in a similar fashion. For consistency with the present simulations all the runs are repeated here with the full three-dimensional model thus yielding the additional information on the maximum concentrations on the arcs and the average plume width.

When performing the 'urban' simulations, Equation (1) indicates that the Reynolds stress profile is well defined only above the zero plane displacement height. Indeed, in the present 'urban' simulations a vertical domain in $z' = z - d$ is used,

i.e., the ground is assumed at $z' = 0$. Unfortunately, the information from the three tracer experiments does not contain a value for d , so that this parameter has to be estimated from other information. The general procedure adopted for this task is as follows. Given the average building height h and a roughness length z_o (both being available from the original data reports, see below) the ratio z_o/h is used to infer a fraction of built-up area A_r/A , where A_r is the built-up area and A is the total area in the region of the release. This is done by (inversely) using a functional relation between z_o/h and A_r/A . Once A_r/A is known d/h as a function of A_r/A can be used to find d . These functions relating the roughness parameters to the relative built-up area are taken from Grimmond and Oke (1999), based on the methods of Kutzbach (1961) and Counihan (1971), respectively. Therefore, for a given z_o/h two values for d can be derived, which are, for the three tracer experiments under consideration, considerably different. It is difficult to decide which of the methods is superior (neither is based on full-scale urban observations). Rotach (1994) reports much better correspondence to an independent, turbulence based method (TVM) for d when using the Kutzbach approach, but no information on z_o is given there. Grimmond and Oke (1999), in their comprehensive comparison study of morphological methods to derive z_o and d , find that among the two methods no clear preference can be given: one is slightly advantageous for d , the other one somewhat superior for z_o . Due to this uncertainty the present ‘urban’ simulations are repeated for the two possible values of d , that according to the Kutzbach and that according to the Counihan method. In Section 6 the respective better results will be presented, but in none of the three experiments would the choice for the ‘other’ value of d change any of the conclusions.

In all the simulations (‘urban’ or ‘non-urban’) the available observations of velocity variances or mean wind speed at certain heights are used to scale the respective parameterised profiles in order to optimally match the measurements at the height(s) of observation. However, in order to circumvent giving too much weight to possible (single) erroneous measurements, the scale factors are constrained between [0.666; 1.5].

5.1. SET UP AND ASSUMPTIONS FOR THE COPENHAGEN SIMULATIONS

Details of the Copenhagen tracer experiment can be found in Gryning and Lyck (1984). Nine tracer releases from $z_s = 115$ m were realised under conditions of forced convection over suburban Copenhagen (DK). Measurements of mean wind speed, $\overline{v'^2}$ and $\overline{w'^2}$ are available at the source height, as well as the mixing height z_i from radio soundings. From additional wind speed measurements at $z = 10$ m the friction velocity, u_* , and the Obukhov length, L , were determined using similarity relations and a roughness length $z_o = 0.6$ m. The average building height in the ‘path’ of the plumes is $h \approx 6$ m (S. E. Gryning, personal communication). Based on the method of Kutzbach (1961) a zero plane displacement of $d = 4.0$ m was determined as outlined in the previous subsection.

For the present ‘urban’ simulations the height of the roughness sublayer is assumed at $z_* = 2h$, i.e., the minimum from the range as given by Raupach et al. (1991). Thus, the friction velocity as provided with the data set stems from within the RS. Equation (1) is therefore used to estimate the IS friction velocity, u_*^{IS} , at the height $z'_* = 2h - d$ from the ‘measured’ friction velocity at $z' = 10 - d$ (units of metres). The so estimated u_*^{IS} are about three percent larger than those provided with the data set.

5.2. SET UP AND ASSUMPTIONS FOR THE LILLESTRØM SIMULATIONS

The nine tracer release experiments took place during (strongly) stable or near-neutral conditions over suburban Lillestrøm (N). Here, only those experiments with a defined friction velocity are considered, i.e., the experiment from February 9, 1987, 1015 hours is discarded. This leads to a total of seven experiments with 20 data points (arcs). Measurements of u_* , L , and wind speed at a height of $z = 10$ m are available for all the tracer releases. In addition, the velocity variances (and again wind speed) were observed at the release height of $z_s = 36$ m above ground. All these measures are input to the model in order to determine the stability for the experiment under consideration and to scale the parameterised profiles of wind speed and the velocity variances. For the ‘urban’ simulations the zero plane displacement was estimated using the values of the roughness length, $z_o = 0.5$ m, and the average building height, $h = 8$ m, as provided with data set (Haugsbakk and Tønnesen, 1989). The method of Kutzbach (1961) was used to determine $d = 3.9$ m from z_o and h . No measurement of the boundary-layer height, z_i , was performed during the tracer release experiments. Therefore, z_i is estimated for the present purpose from (Zilitinkevich, 1972)

$$z_i = \text{const.} \cdot \left(\frac{u_* L}{f} \right)^{1/2}, \quad (4)$$

where f is the Coriolis parameter and the proportionality constant is taken to be 0.28 (Lenschow et al., 1988). Again, the height of the roughness sublayer is assumed as $z_* = 2h$ and for the ‘urban’ simulations the measured friction velocity (at $z = 10$ m) is diagnosed as stemming from within the RS. The inertial sublayer friction velocity, u_*^{IS} is found from Equation (1) and with the length scales above to be approximately 14% larger than the measured friction velocity.

5.3. SET UP AND ASSUMPTIONS FOR THE INDIANAPOLIS SIMULATIONS

These tracer release experiments were realised by adding the tracer to the exhaust gas of a power plant situated near downtown Indianapolis (TRC, 1986). Measurements of wind speed, temperature and turbulence statistics are available from a nearby site with a nominal measurement height of 11 m above ground. In addition, the wind speed was determined at 94 m above ground, again at a site not too far

from the source, and the boundary layer height was determined from minisonde profiles for each of the experiments. The source was $z_s = 83.8$ m above ground, but the effective source height due to plume rise was often much higher (see below). The average height of buildings in the upwind area of the urban meteorological site was determined rather crudely from manually 'digitising' Figure 2-1 of TRC (1986), which leads to $h = 12.1$ m, and a ratio $A_r/A = 0.18$. From this, the zero plane displacement was estimated after the Kutzbach method as $d = 8.0$ m, while $z_o = 1.2$ m, which latter value is close to the estimate as provided with the data set (1 m). Based on z_o and d and the assumed $z_* = 2h$, the friction velocity of the inertial sublayer, u_*^{IS} , was determined for the 'urban' simulations in the same fashion as described in the previous subsections. However, due to the relatively low observation height for Reynolds stress when compared to the zero plane displacement, the increase in the friction velocity is approximately 61%, i.e., $u_*^{\text{IS}} = 1.61u_*^{\text{mea}}$.

For both the 'non-urban' and the 'urban' simulations in the present study, the meteorological input to the model is directly taken from the observed turbulence statistics (i.e., the parameterised values for u_* , L , ... provided with the data set and derived after Hanna and Chang (1993) are not used in the present simulations). Plume rise is taken into account by calculating the effective source height for each run individually following Briggs (1984) for stable, neutral and convective stratification, respectively. This leads to an average effective release height of 388 m (given here for the urban simulations. Note, however, that due to turbulence parameters entering the plume-rise formulations, the effective source height is usually higher for the 'non-urban' simulations).

A total of 27 tracer release experiments was selected from the data set, based on the following criteria:

- Quality 3 data only (i.e., highest quality tag);
- All meteorological input variables (Reynolds stress, turbulent heat flux, wind speed, velocity variances, boundary layer height) are available;
- At least one arc with observations of *all* the surface concentration characteristics (CIC, ArcMax, and SigY) is available.

All together, from these 27 releases a total of 85 measurements of each of the characteristics (CIC, ArcMax, SigY) is available for comparison with the simulations. Out of these, seven (with 11 complete arcs) are from stable conditions and the remaining from unstable stratification.

6. Results

In this section, the summary statistics of the 'urban' and 'non-urban' simulations are compared. These are

- Corr the correlation between simulated and measured concentrations;
 FB: the fractional bias $FB = (\bar{C}_{\text{obs}} - \bar{C}_p) / [0.5(\bar{C}_{\text{obs}} + \bar{C}_p)]$;
 NMSE: the normalised mean square error $NMSE = (\bar{C}_{\text{obs}} - \bar{C}_p)^2 / (\bar{C}_{\text{obs}} \cdot \bar{C}_p)$;
 F2: the percentage of simulations within a factor of two of the observations.

Here, C_p is the predicted concentration or length (ArcMax, CIC or SigY), and C_{obs} the observed value. Overbars indicate an average over the respective data set. The significance of differences between the ‘urban’ and ‘non-urban’ simulations in terms of Corr, FB and NMSE is estimated using the seductive bootstrap resampling method after Hanna (1989). Thereby, 1000 samples of possible pairs $C_{p,\text{urban}} - C_{p,\text{non-urban}}$ are considered for each data set, and 95% confidence limits are based on the 2.5% and 97.5% quantiles of the distribution of statistics from the 1000 samples.

6.1. COPENHAGEN

The results for the Copenhagen experiment are summarised in Table IIA. Over all, both types of simulation (‘urban’ and ‘non-urban’) have satisfying summary statistics with relatively small fractional biases and normalised mean square errors. Despite the relatively large source height, for which only a small difference between ‘urban’ and ‘non-urban’ simulations can be expected (Rotach, 1999), the ‘urban’ simulation is always better than the ‘non-urban’ one. However, only one of the summary statistics shows a significant difference between the two simulations (Table IIA). Still, if the turbulence structure of the RS is properly taken into account, the mean bias is reduced at the same time as the normalised mean square error is also diminished. This indicates that the ‘urban’ simulation more realistically reproduces the physics of the dispersion process above an urban surface.

If the Counihan approach is used to determine d (Section 5) rather than the method after Kutzbach a relatively small value, $d \approx 0.9$ m, results, which is outside the range of ‘reasonable limits’ as proposed by Grimmond and Oke (1999) for urban roughness parameters. Nevertheless, the corresponding simulations of the Copenhagen data set were performed using this d (Table IIB). The results for CIC in this ‘urban’ simulation are even better than when using the Kutzbach- d , while for ArcMax and SigY the results of the two simulations are similar. Over all, the (more realistic) value for d (after Kutzbach) leads to somewhat better summary statistics, but both ‘urban’ simulations are superior to the ‘non-urban’ set-up and support the idea of an improved physical representation of dispersion characteristics when including roughness-sublayer turbulence.

As a second input parameter, for which no observational evidence is available from the original data set, the height of the roughness sublayer, z_* is considered. If $z_* = 3h$ is assumed, ‘urban’ summary statistics are still better than their ‘non-urban’ counterpart for CIC, while for ArcMax and SigY the results are less clear.

TABLE IIA

Comparison of summary statistics for the Copenhagen data set. The total number of data points is 23. The zero plane displacement is determined after the method of Kutzbach (1961), $d = 4$ m. Light shading highlights the simulation performing better. Dark shading indicates a significant difference between 'urban' and 'non-urban' simulations at the 95% level according to seductive bootstrap resampling (Hanna, 1989).

	CIC		ArcMax		σ_y	
	'non-urban'	'urban'	'non-urban'	'urban'	'non-urban'	'urban'
Corr	0.839	0.889	0.909	0.917	0.825	0.845
FB	0.200	0.188	0.311	0.301	−0.065	−0.059
NMSE	0.126	0.100	0.217	0.199	0.06	0.05
F2 [%]	96	100	78	87	100	100

TABLE IIB

As Table IIA, but the zero plane displacement is determined after the method of Counihan (1971), $d = 0.9$ m. The total number of data points is 23. Light shading highlights the simulation performing better. Dark shading indicates a significant difference between 'urban' and 'non-urban' simulations at the 95% level according to seductive bootstrap resampling (Hanna, 1989).

	CIC		ArcMax		σ_y	
	'non-urban'	'urban'	'non-urban'	'urban'	'non-urban'	'urban'
Corr	0.839	0.874	0.909	0.865	0.825	0.866
FB	0.200	0.119	0.311	0.211	−0.065	−0.163
NMSE	0.126	0.078	0.217	0.228	0.06	0.075
F2 [%]	96	100	78	78	100	100

FB and F2 become much better than the values of Tables IIA and IIB but on the other hand, the correlation coefficient and the NMSE are worse even than in the 'non-urban' simulation (not shown). Thus, for a relatively large (assumed) vertical extension of the RS it seems that the good performance of the average statistics (bias) can only be realised at the expense of an enhanced scatter. In addition, when comparing the parameterised values of mean wind speed and the velocity variances with the observations (Section 5), much better correspondence is obtained for $z_* = 2h$ than for $z_* = 3h$ (note that this difference does not affect the respective 'urban' simulation results due to the scaling as described in Section 5). It may be concluded, therefore, that the present 'urban' simulations (Table IIA) yield some indirect evidence for a z_* value at the lower end of the range given by Raupach et al. (1991).

The results as presented in Tables II are similar concerning the general features to those from a simulation with a two-dimensional LSPDM (Rotach and de Haan,

TABLE IIIA

Comparison of summary statistics for the Lillestrøm data set. The total number of data points is 20. Light shading highlights the simulation performing better. Note that there is no dark shading (due to missing significant differences) as in Tables II, IV and V.

	CIC		ArcMax		σ_y	
	'non-urban'	'urban'	'non-urban'	'urban'	'non-urban'	'urban'
Corr	0.316	0.177	0.247	0.011	0.663	0.613
FB	0.293	0.128	-0.153	-0.286	0.614	0.597
NMSE	1.075	1.416	0.948	1.811	0.682	0.679
F2 [%]	30	35	55	50	30	40

1997). Only CIC can be compared, of course, and due to the choice of Rotach and de Haan (1997) for the zero plane displacement, Table IIB should be compared to their Table 2. The minor differences in the results from the two-dimensional and three-dimensional simulations are mainly related to the revised formulation for Reynolds stress within the RS (Equation (1)) and a different method to determine the concentration fields (box counting vs. kernel method, see Section 3). Both approaches, however, support the hypothesis that the underestimation of surface concentrations, as reported for many models and model types in the case of the Copenhagen tracer experiment (Tassone et al., 1994; Olesen, 1995; de Haan and Rotach, 1998) is at least partly due to neglecting the turbulence structure of the roughness sublayer.

6.2. LILLESTRØM

In Table IIIA the results for the Lillestrøm experiment from all the seven runs are compiled. The overall statistics ('urban' or 'non-urban') are generally much less satisfying than those from the Copenhagen experiment, showing a low correlation coefficient along with a NMSE of the order of one, and only one third to one half of the predictions within a factor of two of the observations. There is no indication of either simulation ('urban' or 'non-urban') performing better for all four statistics. Inspecting the individual runs, it even turns out that simulated ('urban' or 'non-urban') and observed concentrations as a function of distance are sometimes completely different and this seems to be more often the case if CIC is concerned than for the other variables (Figure 6). Table IIIA also reveals that the ArcMax prediction is particularly bad in the 'urban' simulation. This is entirely due to one single run (that of January 17, 1987, 1015). If this run is excluded from the analysis, the summary statistics completely change (Table IIIB) and so does the ranking between 'urban' and 'non-urban' simulations.

TABLE IIIB

As Table IIIA, but the experiment of 17 January, 1987, 1015 discarded. The total number of data points is 17. Light shading highlights the simulation performing better. Note that there is no dark shading (due to missing significant differences) as in Tables II, IV and V.

	CIC		ArcMax		σ_y	
	'non-urban'	'urban'	'non-urban'	'urban'	'non-urban'	'urban'
Corr	0.556	0.518	0.366	0.390	0.727	0.647
FB	0.647	0.649	0.039	0.134	0.713	0.685
NMSE	1.030	1.089	0.816	0.807	0.850	0.850
F2 [%]	29	41	59	59	24	35

The results from the Lillestrøm experiment presented here ('urban' or 'non-urban') are similar to those from other studies using simpler or equally as sophisticated dispersion models (Olesen, 1995; de Haan and Rotach, 1998). This means that models of any complexity, but all relying on similarity relations to describe the turbulence statistics, fail to reproduce the experimental data, thus indicating that perhaps a regime of intermittent turbulence may have prevailed during these tracer release experiments (S. E. Gryning, 1998, personal communication). Also, plume meandering may have influenced the position of the actual plume under the strongly stable atmospheric conditions, again making predictions with 'traditional' dispersion models difficult.

The sensitivity analysis of Section 4 has indicated that, in principle, the effect of RS turbulence should be largest under stable conditions. However, this is only true if the turbulence state of the boundary layer during the releases corresponds to the underlying assumptions in the employed dispersion model (similarity relations). This is likely not to be the case for the Lillestrøm experiments and hence any systematic difference between the 'urban' and 'non-urban' approaches seems to be masked by the complicated turbulence state.

6.3. INDIANAPOLIS

The results for Indianapolis are summarised in Table IVA. Again, the overall performance of both models is worse than for the Copenhagen experiment, but clearly better than for Lillestrøm. With one exception, all the statistics from the 'urban' simulations are better than those from the 'non-urban' ones, and some of the differences are even significant at the 95% confidence level. The relatively minor improvement of the 'urban' simulations is due to the high effective release heights because of plume rise (Section 5.3). If only the unstable runs are considered, both the overall model performance as well as the improvement due to roughness-sublayer turbulence ('urban' vs. 'non-urban') is clearly enhanced (Table IVB).

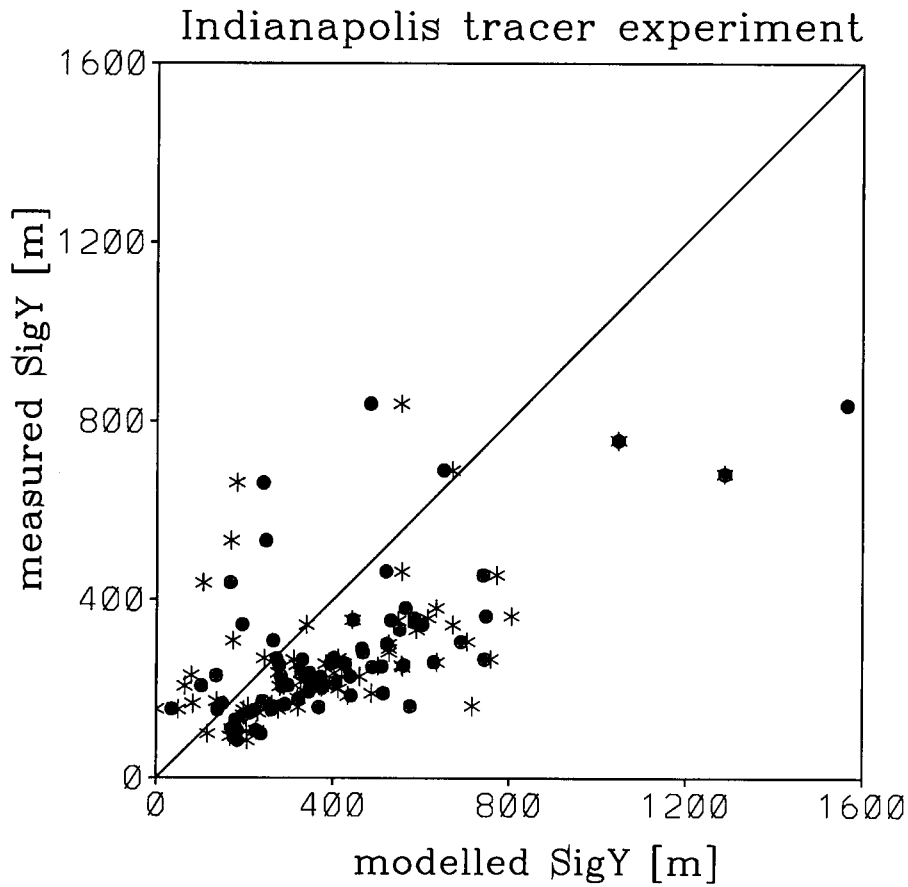


Figure 7. Modelled vs. observed SigY for the unstable runs of the Indianapolis tracer experiment. Full dots: 'urban' simulation, stars: 'non-urban' simulation.

The group of unstable runs is characterised by z_i/L values ranging from -3 to 'minus infinity' with the majority of runs having $z_i/L > -10$. For these unstable runs alone, the 'urban' simulations are clearly, and for NMSE and FB (not CIC) significantly, superior to the 'non-urban' set-up (Figure 7 as an example), although they still do not reach the quality of the Copenhagen results (for possible reasons, see the discussion below). In turn, the summary statistics for the stable runs alone are similar to those from the Lillestrøm experiment in both their absolute performance (low correlation coefficients, NMSE of order one, F2 of about 30%) and the missing preference for either the 'urban' or the 'non-urban' set-up (not shown).

Plume rise uncertainties may be responsible for the relatively poor model performance (irrespective of whether 'urban' or 'non-urban' simulations are considered). To explore this possibility we may define the fractional bias of the individual observations as a function of distance from the source, i.e., $FB_i(x) = C_{\text{obs},i} - C_{p,i} / [0.5(C_{p,i} + C_{\text{obs},i})]$. Here, the subscript 'i' refers to a single measure-

TABLE IVA

Comparison of summary statistics for the Indianapolis data set. The total number of data points is 85. Light shading highlights the simulation performing better. Dark shading indicates a significant difference between 'urban' and 'non-urban' simulations at the 95% level according to seductive bootstrap resampling (Hanna, 1989).

	CIC [mg m^{-2}]		ArcMax [$\mu\text{g m}^{-3}$]		σ_y [m]	
	'non-urban'	'urban'	'non-urban'	'urban'	'non-urban'	'urban'
Corr	0.525	0.553	0.376	0.240	0.659	0.674
FB	0.270	0.257	0.687	0.621	-0.399	-0.357
NMSE	0.651	0.485	1.377	1.248	0.533	0.404
F2 [%]	45	58	40	44	71	79

TABLE IVB

Comparison of summary statistics for the Indianapolis data set. Only unstable runs considered. The total number of data points is 72. Light shading highlights the respective better performing simulation. Dark shading indicates a significant difference between 'urban' and 'non-urban' simulations at the 95% level according to seductive bootstrap resampling (Hanna, 1989).

	CIC [mg m^{-2}]		ArcMax [$\mu\text{g m}^{-3}$]		σ_y [m]	
	'non-urban'	'urban'	'non-urban'	'urban'	'non-urban'	'urban'
Corr	0.568	0.618	0.224	0.250	0.660	0.685
FB	-0.273	0.251	0.691	0.564	-0.398	-0.334
NMSE	0.611	0.416	1.418	0.997	0.527	0.387
F2 [%]	46	62	38	45	71	81

ment of quantity C (CIC, ArcMax or SigY) at a particular arc and in a particular release, rather than the average as defined in the beginning of Section 6. Figure 8 shows that the model performs worse close to the source and improves with increasing distance. Thus, due to having employed effective release heights rather than trying to simulate a continuously lifting plume in a Lagrangian framework (e.g., Heinz and van Dop, 1999), the surface concentrations close to the source are often severely underpredicted (large positive FB for CIC and ArcMax and also large NMSE, see Table IVB). This deficiency will have to be addressed in the future in order to obtain better overall predictions.

As for the Copenhagen data set some sensitivity tests were performed concerning the most speculative input parameters for the 'urban' simulation, namely d and z_* . Again, instead of using the approach of Kutzbach (1961) to determine d the approach of Counihan (1971) may be used. Due to the fact, however, that the ratio A_r/A is explicitly available for the Indianapolis data set (Section 5.3) a fair comparison between the two approaches will use both d and z_o according to the same

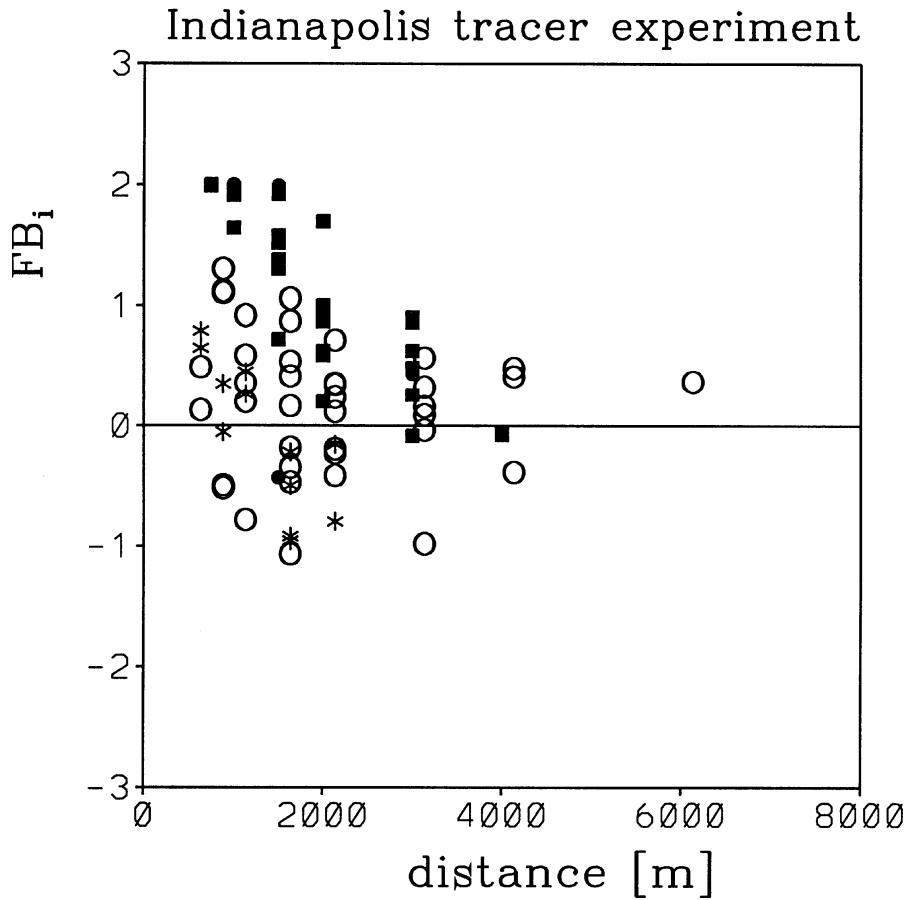


Figure 8. Individual fractional bias, FB_i , of CIC from the Indianapolis data set as a function of the distance from the source. ■: $z_s > 600$ m, ●: $400 \text{ m} < z_s < 600$ m, ○: $250 \text{ m} < z_s < 400$ m, *: $z_s < 250$ m.

method. If the Counihan approach is used for the urban surface of Indianapolis a roughness length $z_o = 2$ m is obtained, while $d = 2.7$ m results. These values, although quite unrealistic for a mean building height of roughly 12 m, were used in an additional simulation for the ‘non-urban’ and ‘urban’ set-ups, respectively. The results (Table V) show that again the ‘urban’ simulation generally performs better than the ‘non-urban’ one. This is partly due to the very bad performance of the ‘non-urban’ simulation with this large value of z_o . However, comparing Tables IVA and V also reveals that the two ‘urban’ results are comparable, thus indicating that there is no severe influence of the (uncertain) value of d . For CIC and ArcMax the summary statistics from the ‘urban’ simulation with the ‘Counihan- d ’ are even slightly better than those using the ‘Kutzbach- d ’, while the opposite holds true for SigY.

TABLE V

Comparison of summary statistics for the Indianapolis data set when d and z_o are determined after the method of Counihan (1971). All runs (stable and unstable) considered. The total number of data points is 85. Light shading highlights the respective better performing simulation. Dark shading indicates a significant difference between ‘urban’ and ‘non-urban’ simulations at the 95% level according to seductive bootstrap resampling (Hanna, 1989).

	CIC [mg m^{-2}]		ArcMax [$\mu\text{g m}^{-3}$]		σ_y [m]	
	‘non-urban’	‘urban’	‘non-urban’	‘urban’	‘non-urban’	‘urban’
Corr	0.046	0.588	−0.090	0.241	0.654	0.677
FB	−0.127	0.167	−0.147	0.536	−0.492	−0.420
NMSE	3.308	0.373	16.641	1.190	0.670	0.443
F2 [%]	54	61	39	44	54	76

If $z_* = 3h$ is used in the ‘urban’ simulation the results are very similar to those of Table IVA (not shown). Some of the summary statistics improve (mainly those for ArcMax) and others become worse. Most of them (with the exception of Corr for CIC and FB for SigY), however, still remain better than those of the ‘non-urban’ simulation. It therefore appears that no definitive preference can be given for z_* (at this site) based on the present simulations.

In summary, for the Indianapolis data set we can state that the ‘urban’ simulations show an improvement in the summary statistics over the ‘non-urban’, irrespective of the ‘choice’ of values for the critical input parameters d and z_* . This improvement is solely due to the near-neutral and unstable runs, and indicates that at least in this stability range the physical process of dispersion is better taken into account in the ‘urban’ set-up, than it is in the ‘traditional’, i.e., ‘non-urban’, approach. The overall performance of the simulations (‘urban’ *or* ‘non-urban’) is not optimal due to the treatment of plume rise in the present simulations, which asks for improvement.

7. Summary and Conclusions

A modelling approach is presented for urban-scale dispersion of chemically inert air pollutants. It is argued that it is important to properly take into account the turbulence structure of the roughness sublayer (RS), i.e., the lowest few times the average obstacle height. Based on the (few) available full-scale observations a parameterisation for the vertical profile of Reynolds stress within the roughness sublayer is proposed, which constitutes the key feature of turbulence within this height range. Local scaling (Rotach, 1993b) is then used in combination with this Reynolds stress profile to define an ‘urban’ type of dispersion simulation. In contrast, the term ‘non-urban’ dispersion simulation is employed here for the

traditional approach, which is frequently adopted over urban surfaces by simply specifying a relatively large value for the roughness length. Note that 'non-urban' in this sense must not be mixed up with 'rural' – it only means that the turbulence structure of the RS is not taken into account.

Using a Lagrangian stochastic particle model, 'urban' and 'non-urban' simulations are compared for different stratification and source configurations. Not surprisingly, it is found that the importance of the RS is largest (i.e., differences between 'urban' and 'non-urban' simulations are most pronounced) for mechanically dominated turbulence (near-neutral, stable stratification), for low sources and for an assumed large vertical extension of the RS. This is important insofar as low sources are fairly typical of urban environments on the one hand, and the rough urban surface tends to neutralise the stratification of the boundary layer due to the excessive surface drag on the other hand. For sources well above the RS and/or unstable stratification, differences are found to be smaller (some twenty percent at maximum) but the 'urban' simulations consistently yield somewhat larger surface concentrations. In the light of frequently encountered underestimations of surface concentrations in urban dispersion studies (e.g., Tassone et al., 1994; Olesen, 1995; de Haan and Rotach, 1998) this suggests that the present 'urban' approach is likely to improve the predictability by explicitly taking into account the turbulence structure of the RS.

Clearly, the above results call for a tracer experiment with *low source height* and *mechanically dominated* turbulence conditions to thoroughly validate the 'urban' approach proposed here. However, to the knowledge of the author no such tracer experiment is available from the open literature. Therefore, 'urban' and 'non-urban' simulations are compared for the three tracer-release experiments in Copenhagen, Indianapolis and Lillestrøm. The former two are characterised by relatively large source heights over a suburban and an urban surface, respectively, while the latter was performed under extremely stable conditions with all the associated possible problems of plume meandering and intermittent turbulence.

For unstable stratification the results show that in the 'urban' simulations the fractional bias and the normalised mean square error are simultaneously reduced as compared to the 'non-urban' simulations. In the case of the Indianapolis experiment, some of the summary statistics are even significantly better in the 'urban' simulation at the 95% confidence level (Hanna 1989). This demonstrates that, (i) the influence of roughness-sublayer turbulence is non-negligible over urban surfaces (see below), and (ii) that the chosen approach captures the essential characteristics of the dispersion process in this height range. For releases under stable stratification it is found that the uncertainty of the dispersion simulation as such (due to inappropriate similarity assumptions for the situations during the tracer releases or due to plume meandering) is so large that any possible improvement due to the 'urban' modification is masked.

In absolute terms most of the summary statistics for the 'urban' simulations of the three tracer experiments are only slightly better than the respective 'non-urban'

ones. While the correlation coefficient is increased by typically a few percent, the other summary statistics improve by typically between 10 and 20 percent (only for the unstable runs, see above). This relatively small improvement is mainly due to the large source height in the Copenhagen and Indianapolis tracer experiments ($z_s/h = 19$ and $z_s/h = O(30)$ respectively), so that only a minor part of the diffusion process is affected by the roughness sublayer. It is important, however, to note that the 'urban' approach improves the correlation to observations, the fractional bias, the mean scatter and the 'factor of two', all at the same time and for some of the statistics significantly. Thus, the present 'urban' approach is not a mere 'tuning' in order to resolve the generally encountered underestimation of surface concentrations when modelling for example the Copenhagen data with different models (e.g., Olesen, 1995). Rather, it shows that more of the physics of the actual dispersion process are taken into account in the 'urban' simulation.

De Haan et al. (2000) use the same approach of 'urban' simulations for simulating yearly average surface concentrations of NO_x and SO_2 in the city of Zurich (Switzerland). In this study, a Gaussian plume model is used in combination with a detailed emission inventory. The underestimation by the 'non-urban' simulation of the annual mean surface concentration, as observed at 28 stations, is found to be considerably reduced in the 'urban' approach. The increase by about 30% in surface concentrations reflects the effect of the present 'urban' approach in a case with typical, i.e., low, source heights from traffic and domestic heating in a city environment. Clearly, more observational data and, in particular, a tracer experiment over an urban surface with a relatively low source height will be highly desirable in order to further explore the potential of the present 'urban' approach to air pollution modelling over cities.

Acknowledgements

The author is indebted to one of the anonymous reviewers whose instrumental comments and suggestions greatly improved the present paper. This work was conducted in the framework of a research project financed by the Swiss National Science Foundation (grant 21-46849.96).

References

- Briggs, G. A.: 1984, 'Plume Rise and Buoyancy Effects', in D. Randerson (ed.), *Atmospheric Science and Power Production*, Tech. Information Center, DOE/ TIC 27601, pp. 327–366.
- Clarke, C. F., Ching, J. K. S., and Godowich, J. M.: 1982, *A Study of Turbulence in an Urban Environment*, EPA Technical Report, EPA 600-S3-82-062.
- Counihan, J.: 1971, 'Wind Tunnel Determination of the Roughness Length as a Function of the Fetch of Three-Dimensional Roughness Elements', *Atmos. Environ.* **5**, 637–642.
- Du, S.: 1997, 'Universality of the Lagrangian Velocity Structure Function Constant (Co) Across Different Kinds of Turbulence', *Boundary-Layer Meteorol.* **83**, 207–219.

- Du, S., Sawford, B. L., Wilson, J. D., and Wilson D. J.: 1995, 'Estimation of the Kolmogorov Constant (Co) for the Lagrangian Structure Function, Using a Second Order Lagrangian Model of Grid Turbulence', *Phys. Fluids* **7**, 3083–3090.
- Feigenwinter, C., Vogt, R., and Parlow, E.: 1999, 'Vertical Structure of Selected Turbulence Characteristics above an Urban Canopy', *Theor. Appl. Clim.* **62**, 51–63.
- Grimmond, C. S. B. and Oke, T. R.: 1999, 'Aerodynamic Properties of Urban Areas Derived from Analysis of Surface Form', *J. Appl. Meteorol.* **38**, 1262–1292.
- Gryning, S.-E. and Lyck, E.: 1984, 'Atmospheric Dispersion from Elevated Sources in an Urban Areas: Comparison between Tracer Experiments and Model Calculations', *J. Clim. Appl. Meteorol.* **23**, 651–660.
- de Haan, P.: 1999, 'On the Use of Density Kernels for Concentration Estimations Within Particle and Puff Dispersion Models', *Atmos. Environ.* **33**, 2007–2021.
- de Haan, P. and Rotach, M. W.: 1998, 'A Novel Approach to Atmospheric Dispersion Modelling: The Puff-Particle Model (PPM)', *Quart. J. Roy. Meteorol. Soc.* **124**, 2771–2792.
- de Haan, P., Rotach, M. W., and Werfeli, M.: 1998, 'Extension of an Operational Short-Range Dispersion Model for Application in Urban Environments', *Int. J. Vehicle Design* **20**, 105–114.
- de Haan, P., Rotach, M. W., and Werfeli, M.: 2000, 'Extension of the OML Dispersion Model to Urban and Near-Source Applications', *J. Appl. Meteorol.*, in press.
- Hanna, S. R.: 1982, 'Applications in Modelling', in F. T. M. Nieuwstadt and H. van Dop (eds.), *Atmospheric Turbulence and Air Pollution*, Reidel Publishing Company, Dordrecht, 358 pp.
- Hanna, S. R.: 1989, 'Confidence Limits for Air Quality Model Evaluations, as Estimated by Bootstrap and Jackknife Resampling Methods', *Atmos. Environ.* **23**, 1385–1398.
- Hanna, S. R. and Chang, J. C.: 1993, 'Hybrid Plume Dispersion Model (HPDM). Improvements and Testing at Three Field Sites', *Atmos. Environ.* **27A**, 1491–1508.
- Haugsbakk, I. and Tønnesen, D. A.: 1989, *Atmospheric Dispersion Experiments at Lillestrøm 1986–1987*. Data Report, NILU, OR 41/89.
- Heinz, S. and van Dop, H.: 1999, 'Buoyant Plume Rise Described by a Lagrangian Turbulence Model', *Atmos. Environ.* **33**, 2031–2043.
- Högström, U., Bergström, H., and Alexandersson, H.: 1982, 'Turbulence Characteristics in a Near-Neutrally Stratified Urban Atmosphere', *Boundary-Layer Meteorol.* **23**, 449–472.
- Kono, H.: 1997, 'Modelling the Dispersion of Motor Vehicle Exhaust Gases, Including Building Effects, and its Application to the Calculation of NO_x Concentration in Osaka City', *Int. J. Environ. Poll.* **8**, 620–627.
- Kutzbach, J.: 1961, *Investigations of the Modifications of Wind Profiles by Artificially Controlled Surface Roughness. Studies of the Three-Dimensional Structure of the Planetary Boundary Layer*, Annual Report, Dept. of Meteorology, Univ. of Wisconsin, Madison.
- Lenschow, D. H., Zhang, S. F., and Stankow, B. B.: 1988, 'The Stably Stratified Boundary Layer over the Great Plains I: Mean and Turbulence Structure', *Boundary-Layer Meteorol.* **42**, 95–122.
- Luhar, A. L. and Britter, R. E.: 1989, 'A Random Walk Model for Dispersion in Inhomogeneous Turbulence in a Convective Boundary Layer', *Atmos. Environ.* **23**, 1911–1924.
- Martilli, A., Clappier, A., and Rotach, M. W.: 2000, 'A Parameterisation of the Urban Effects for Mesoscale Models', in *Preprints of the 3rd Symposium on the Urban Environment*, 14–18 August 2000, Davis, CA, pp. 131–132.
- Martilli, A., Clappier, A., Calpini, B., Van den Bergh, H., and Krueger, B. C.: 1997, 'Passive Tracer Studies with the Model CTC for the Athens 2004 Project', in N. Moussiopoulos and S. Papagrigoriou (eds.), *Proceedings of the International Scientific Workshop 'Athens 2004 Air Quality Study*, Athens 18/19 February, pp. 83–94.
- Nieuwstadt, F. T. M.: 1984, 'The Turbulence Structure of the Stable Nocturnal Boundary Layer', *J. Atmos. Sci.* **41**, 2202–2216.
- Oikawa, S. and Meng, Y.: 1995, 'Turbulence Characteristics and Organized Motion in a Suburban Roughness Sublayer', *Boundary-Layer Meteorol.* **74**, 289–312.

- Olesen, H. R.: 1995, 'The Model Validation Exercise at Mol: Overview of Results', *Int. J. Environ. Poll.* **5**, 761–784.
- Rafailidis, S.: 1997, 'Influence of Building Areal Density and Roof Shape on the Wind Characteristics Above a Town', *Boundary-Layer Meteorol.* **85**, 255–271.
- Raupach, M. R., Antonia, R. A., and Rajagopalan, S.: 1991, 'Rough-Wall Turbulent Boundary Layers', *Appl. Mech. Rev.* **44**, 1–25.
- Rotach, M. W.: 1991, *Turbulence within and above an Urban Canopy*, ETH Diss. 9439, 240 pp., Published as ZGS, Heft 45, Verlag GIETH, Zürich.
- Rotach, M. W.: 1993a, 'Turbulence Close to a Rough Urban Surface Part I: Reynolds Stress', *Boundary-Layer Meteorol.* **65**, 1–28.
- Rotach, M. W.: 1993b, 'Turbulence Close to a Rough Urban Surface Part II: Variances and Gradients', *Boundary-Layer Meteorol.* **66**, 75–92.
- Rotach, M. W.: 1994, 'Determination of the Zero Plane Displacement in an Urban Environment', *Boundary-Layer Meteorol.* **67**, 187–193.
- Rotach, M. W.: 1995, 'Profiles of Turbulence Statistics in and above an Urban Street Canyon', *Atmos. Environ.* **29**, 1473–1486.
- Rotach, M. W.: 1997a, 'The Turbulence Structure in an Urban Roughness Sublayer', in R. J. Perkins and S. E. Belcher (eds.), *Flow and Dispersion through Groups of Obstacles*, Clarendon Press, Oxford, pp. 143–155.
- Rotach, M. W.: 1997b, 'Towards a Meteorological Preprocessor for Dispersion Models in an Urban Environment', *Int. J. Environ. Poll.* **8**, 548–556.
- Rotach, M. W.: 1997c, 'The Effect of Urban Roughness Sublayer Turbulence on Dispersion', in *Preprints 12th Symposium on Boundary Layers and Turbulence*, July 28–August 1, 1997, Vancouver, BC, Canada, pp. 453–454.
- Rotach, M. W.: 1999, 'On the Urban Roughness Sublayer', *Atmos. Environ.* **33**, 4001–4008.
- Rotach, M. W. and de Haan, P.: 1997, 'On the Urban Aspect of the Copenhagen Data Set', *Int. J. Environ. Poll.* **8**, 279–286.
- Rotach, M. W., Gryning, S. E., and Tassone C.: 1996, 'A Two-Dimensional Stochastic Lagrangian Dispersion Model for Daytime Conditions', *Quart. J. Roy. Meteorol. Soc.* **122**, 367–389.
- Roth, M.: 2000, 'Review of Atmospheric Turbulence over Cities', *Quart. J. Roy. Meteorol. Soc.* **126**, 1941–1990.
- Roth, M. and Oke, T. R.: 1993, 'Turbulent Transfer Relationships over an Urban Surface. I: Spectral Characteristics', *Quart. J. Roy. Meteorol. Soc.* **119**, 1071–1104.
- Schayes, G., Thunis, P., and Bornstein, R.: 1996, 'Topographic Vorticity-Mode Mesoscale-B (TVM) Model. Part I: Formulation', *J. Appl. Meteorol.* **35**, 1815–1823.
- Schmid, H. P.: 1997, 'Experimental Design for Flux Measurements: Matching Scales of Observations and Fluxes', *Agric. For. Meteorol.* **87**, 179–200.
- Sorbjan, Z.: 1986, 'On Similarity in the Atmospheric Boundary Layer', *Boundary-Layer Meteorol.* **34**, 377–397.
- Tassone, C., Gryning, S.-E., and Rotach, M.W.: 1994, 'A Random-Walk Model for Atmospheric Dispersion in the Daytime Boundary Layer', in S. E. Gryning and M. M. Millan (eds.), *Air Pollution Modelling and its Application X*, NATO, Challenges of Modern Society, Vol. 18, pp. 243–251.
- Thomson, D. J.: 1987, 'Criteria for the Selection of Stochastic Models of Particle Trajectories in Turbulent Flows', *J. Fluid Mech.* **180**, 529–556.
- TRC: 1986, *Urban Power Plant Plume Studies*, EPRI report EA-5468, EPRI, 3412 Hillview Ave., Palo Alto, CA 94304.
- Zilitinkevich, S. S.: 1972, 'On the Determination of the Height of the Ekman Boundary Layer', *Boundary-Layer Meteorol.* **3**, 141–145.